Journal of Biomedical Materials Research Part A

WILEY

Society For Biomaterials

RESEARCH ARTICLE OPEN ACCESS

The Importance of Coating Surface and Composition for Attachment and Survival of Neuronal Cells Under Mechanical Stimulation

Pascal A. M. M. Vroemen[1,2] | Adrián Seijas-Gamardo[1,2] | Roy Palmen[1] | Paul A. Wieringa[2] | Carroll A. B. Webers[1] | Lorenzo Moroni[2] | Theo G. M. F. Gorgels[1]

[1]Maastricht UMC+, Maastricht University Medical Centre+, University Eye Clinic, Maastricht, the Netherlands | [2]MERLN Institute for Technology-Inspired Regenerative Medicine, Maastricht University, Maastricht, the Netherlands

Correspondence: Pascal A. M. M. Vroemen (p.vroemen@maastrichtuniversity.nl)

Received: 22 July 2024 | **Revised:** 9 April 2025 | **Accepted:** 11 April 2025

Funding: This work was supported by Stichting Steunfonds Uitzicht, Glaucoomfonds, Landelijke Stichting voor Blinden en Slechtzienden, Oogfonds, Rotterdamse Stichting Blindenbelangen.

Keywords: coating | glaucoma | laminin | mechanical stimulation | neuronal cells | PC-12 | retinal ganglion cell

ABSTRACT

Cell culture of neuronal cells places high demands on the surface for these cells to adhere to and grow on. Native extracellular matrix (ECM) proteins are often applied to the cell culture surface. The substrate is even more important when mechanical strain is applied to the cells in culture. These cells will easily detach and die, precluding the study of how mechanical factors affect these cells. Mechanical factors are, for example, important in the eye disorder glaucoma, which is characterized by the loss of the retinal ganglion cells (RGCs), the retinal neurons that transfer the visual information from the retina via the optic nerve to the brain. High intraocular pressure is the main risk factor of glaucoma. Here, we aimed to find an optimal coating formulation for mechanical testing of the two cell types that are often used for in vitro studies on glaucoma: primary rat retinal ganglion cells (RGCs) and the neuronal PC-12 cell line. Glass and polymer coverslips as well as well plate wells were coated with various substrates: fibronectin, collagen 1, RGD peptide, polyethyleneimine (PEI), poly-D-lysine (PDL), and laminin. We used a thermomixer for 1 min at 500RPM and 37°C to apply mechanical strain and test cell attachment in medium throughput during mechanical stimulation. Cell density, morphology, and cell death were measured to evaluate the coatings. First, a screen of various surfaces and coatings was performed using PC-12 cells, after which a selection of coating strategies was tested with RGCs. For PC-12 cells, the best results were obtained using a coating with a mixture of 10 μg/mL PDL with 2 or 50 μg/mL laminin in PBS (M2). This resulted in the highest cell density, with and without mechanical stimulation. Many other coating strategies failed to provide an effective substrate for adherence and growth of PC-12 cells. Coating composition as well as coating strategy influenced cell attachment and survival. Contrary to PC-12 cells, RGCs performed better in a sequential coating of first 10 μg/mL PDL and then 2 μg/mL laminin (S2). With this protocol, RGCs showed best neurite growth and highest cell density. Based on this difference between PC-12 cells and RGCs, we conclude that the optimal coating depends on the cell type. When reporting cell culture studies, it is important to fully specify culture surface, surface treatment, and coating protocol since all these factors influence cell attachment, growth, and survival.

1 | Introduction

Human tissues are composed of cells and extracellular matrix (ECM). The ECM gives support to cells and provides necessary cues for proliferation, differentiation, migration, and survival [1, 2]. When cells are cultured in the lab, they are often grown on tissue culture plastic (TCP). These surfaces can be plasma treated to make the polystyrene more hydrophilic, improving adherence of cultured cells. While this approach is adequate to culture a wide variety of cell types, it is not suitable for some cell types, such as neuronal cells. For neuronal cells, standard TCP is too stiff and may fail to provide the correct adhesive ligands present in native ECM [3]. Neuronal cells appear to require an ECM coated surface that better represents the physico-chemical properties of the native tissue environment [4, 5]. Many different coatings, mimicking native ECM, have been used for neuronal cell culture, such as poly-D-lysine (PDL) and laminin. Other frequently used coatings are collagen, fibronectin, polyethyleneimine (PEI), and poly-L-lysine [6–11]. Besides plastic, glass coverslips are used as surfaces for substrate coating to culture neuronal cells [10].

Such ECM- and synthetic-coated substrates can be very useful when establishing in vitro models to further deepen our understanding of glaucoma, where elevated intraocular pressure is an important risk factor. This suggests that mechanical strain plays an important role in the pathology [12]. Glaucoma is characterized by the death of retinal ganglion cells (RGCs), the retinal neurons that project their axons through the optic nerve to the brain [13]. In order to analyze the mechanical aspects of RGC death, we simulate this mechanical strain in vitro [14]. In pilot experiments applying pressure to primary rat RGCs and the neuronal PC-12 cell line in vitro, we noticed that many cells detach in these mechanical strain conditions, making a detailed analysis of the relevant cell biological events difficult. Therefore, we performed this study aiming to find an optimal coating for these in vitro model experiments.

Many different coatings have been reported in the literature to culture RGCs. Most often, a combination of PDL and laminin is used, but this coating is not standardized in terms of coating protocol and concentrations of the components [15–33]. In addition, coating protocols are often incompletely reported: for example, laminin concentration is frequently not reported, or the concentration is reported, but not the coating protocol (layer-by-layer coating or mixed in a buffer). Currently, it is unclear which coating is best for the two cell types that are of most interest for glaucoma in vitro models: primary rat RGCs and the PC-12 cell line, used as a neuronal cell model [34, 35]. The present study aimed to find a coated surface that allows RGCs to grow well and remain attached both under normal conditions and under mechanical strain comparable to conditions occurring in glaucoma. As a reproducible method of mechanical stimulation, we used a thermomixer with the following settings: 500RPM for 1 min at 37°C. Various surfaces and a variety of coatings reported in the literature were tested. We first screened a wide spectrum of coatings with the neuronal cell line PC-12. After this, a selection was tested with primary rat RGCs. The readouts were cell density, cell death, and morphology. As mentioned above, it is our aim to find a suitable substrate to which the cells would attach and remain available for future research. We chose this method not as a mimic for glaucoma, but as a reproducible method for mechanical stimulation that challenges the adhesion.

2 | Methods

2.1 | Surfaces

We chose three different surfaces for our study, that is, glass coverslips, Ibidi polymer coverslips, and polystyrene wells. A 12 mm (diameter) Menzel glaser #0 coverslip (Lot 0589 Thermo Scientific) was either washed with 70% ethanol in a 50 mL tube under constant agitation of a roller bench for >1 month (ethanol was refreshed every 2–3 days to ensure optimal cleaning) or piranha-etched for 50 min in a glass beaker with piranha solution (3:1 sulfuric acid/hydrogen peroxide) while stirred regularly. Etched coverslips were washed afterward and stored in 70% ethanol until use. Uncoated #1.5 Ibidi polymer coverslips (25 mm × 75 mm, Ibidi 10,813) were manually punched to 12 mm coverslip size and stored in 70% ethanol until used. Lastly, untreated tissue culture plastic of 24-well plates (Falcon 24-well Polystyrene Clear Flat Bottom Not Treated Cell Culture Plate 351,147) was used as the coating surface.

2.2 | Coatings

Coverslips were sterilized in 70% ethanol for at least 30 min and rinsed with sterile water (Cell culture grade, 10,001,342, Thermo Fisher) before coating with the different types of compounds and protocols. We chose the following coatings and variations of coatings based on literature and previous experiments: Layer-by-layer (sequential) poly-D-lysine (PDL)/laminin [9, 20, 25, 31–33, 36–39] and polyethyleneimine (PEI)/laminin [7, 9, 40] coatings, or coatings made with a mixture of PDL and laminin [8, 11, 41, 42], as well as commercially available PDL/laminin coated coverslips (BioCoat, Corning 354,087, proprietary formula) [43–46]. We also tested other coatings often used in cell culture, that is, fibronectin [7, 47], collagen 1 [42, 48], and RGD peptide [49]. Lastly, we tested laminin covalently bound to coverslips [50].

We chose three different laminin concentrations in the range of 2–50 μg/mL, as often reported in the literature. Many papers fail to specify coating concentrations [17, 29, 30, 33, 37] and/or do not mention whether laminin was mixed with PDL or applied layer-by-layer [17, 27–30]. We studied both mixed and sequential coating strategies.

For layer-by-layer (sequential) PDL/laminin coating, surfaces (coverslips and wells) were coated with 10 μg/mL poly-D-lysine (PDL, P6407, Sigma-Aldrich) for 30 min in sterile water. Coverslips were then washed three times with sterile water and coated with 2 μg/mL (S2), 20 μg/mL (S20), or 50 μg/mL (S50) laminin (Cultrex 3400-010-02, R&D Systems) in Neurobasal medium by incubating overnight in a 37°C and 5% CO_2 incubator. Coated surfaces were washed three times with Neurobasal medium before cell seeding.

PEI/laminin coating was done using 0.1% polyethyleneimine (PEI, 764604, Sigma-Aldrich) solution diluted in sterile water, incubated overnight at 4°C, followed by three washes with sterile water and coating with 2 μg/mL laminin (PEI 2) or 20 μg/mL laminin (PEI 20) diluted in sterile water, incubated for 1 h at

room temperature. Laminin solutions were removed before cell seeding, without washing.

Mixed PDL/laminin coating was achieved by mixing 10 μg/mL PDL with 2 μg/mL (M2) or 20 μg/mL (M20) laminin in PBS (D8537, Sigma-Aldrich) and incubating this mixture overnight on the surfaces in a 37°C and 5% CO_2 incubator. Coated surfaces were washed three times with PBS before cell seeding. Fibronectin-coated surfaces were made with 0.5 μg/mL fibronectin (F1141, Sigma-Aldrich) in PBS for 1 h. The fibronectin solution was removed just before cell seeding, without washing. Collagen 1 coating was achieved by incubating surfaces with 1 mg/mL rat collagen (354,249, Corning) solution in 0.02 M acetic acid in water overnight at 37°C. Coated surfaces were washed twice with water before cell seeding.

RGD functionalised surfaces were prepared using a combination of silane and thiol-ene click chemistry. The detailed protocol of the RGD surface functionalization is described elsewhere [51]. Briefly, coverslips were washed with ethanol and distilled water, then activated with oxygen plasma treatment (3 min at 60 W). Next, vinyltrimethoxysilane (Sigma) was vapor deposited onto the activated coverslips overnight at 80°C and 100 mbar. Then, a 10 mM CGGGRGDS (Chinapeptides) peptide solution containing 5 mg/mL LAP (Lithium phenyl-2,4,6-trimethylbenzoylphosphinate, TCI chemicals) was dropped onto the vinyl-silane treated surfaces, covered with a fluorinated quartz slide, and irradiated by UV light (254 nm) for 10 min. Finally, the peptide functionalized surfaces were washed with water and ethanol in an ultrasonic bath and stored at 4°C until further use.

Covalent binding of laminin was achieved using an EDC-NHS reaction (ethylene diaminecarbodiimide, N-Hydroxysuccinimide) according to the protocol of Chandradoss et al. [52]. Piranha-etched coverslips were incubated with 1 M KOH overnight at room temperature, followed by amino-silanization with 5% acetic acid and 3% 3-aminopropyl trimethoxysilane (APTES). Functionalization was achieved with 2 μg/mL laminin in 4 mg/mL EDC and 10 mg/mL NHS in milliQ incubated overnight at 4°C. Coverslips were washed with PBS before cell seeding.

2.3 | Cells

Differentiated cells of the rat pheochromocytoma cell line (PC-12; ACC 159, DSMZ, Germany) were used as a model for neuronal cells. PC-12 cells were cultured according to the supplier's protocol. In short, cells were expanded and cultured in growth medium containing 85% RPMI 1640 medium (61870-010, Gibco), 10% horse serum (H1270, Sigma-Aldrich), and 5% heat-inactivated fetal bovine serum (FBS; F7524, Sigma-Aldrich). Cells were dissociated into a single-cell suspension by passing them through a 22-gauge needle several times and treating the cells with trypsin for 5 min. Big clusters of dead cells were removed with a micropipette before seeding. Cells were seeded on coated coverslips or wells in differentiation medium (99% RPMI, 1% horse serum, and 100 ng/mL nerve growth factor (NGF; N1408, Sigma-Aldrich)). We seeded a standard high-density amount of 2.00×10^4 cells per coverslip or well (taking the difference in surface area into account when comparing coverslips and wells) and differentiated for 7 days in a 37°C and 5% CO_2 incubator. Mechanical stimulation was applied (to challenge cell adherence to the coatings) on differentiation day 7.

Primary retinal ganglion cells (RGCs) were isolated from SD-OFA rats (Envigo). All animal procedures were approved by the Central Authority for Scientific Procedures on Animals (CCD, Den Haag, NL, license number AVD107002015334), were approved by the local ethical committee, and were in accordance with the European Directive for animal experiments (2010/63/EU). RGCs were isolated using a combination of immunopanning and magnetic separation. Endothelial cells and microglia were depleted using negative immunopanning according to the protocol of Winzeler and Wang [36, 53]. Positive selection of RGCs was performed with magnetic separation using a Retinal Ganglion Cell Isolation Kit (130-096-209, Miltenyi Biotec) according to the manufacturer's protocol. In brief, P7 rats were decapitated. Retina were removed and dissociated into a single cell suspension using papain digestion and trituration. The retinal single cell suspension was incubated with anti-macrophage antibody and filtered. After filtration, the cell suspension was incubated for two times on a goat anti-rabbit IgG coated immunopanning plate (negative panning). Up to this point, the protocol of Winzeler and Wang [36] was followed with small modifications such as the amount of papain (200 U was used compared to the original 165 U). After negative panning, the suspension of unbound cells was collected and centrifuged at 200 g for 10 min at room temperature. Magnetic labelling was performed according to the protocol of Miltenyi Biotec with a few modifications to accommodate negative selection with a different protocol (immunopanning instead of magnetic depletion). The cell pellet was resuspended in 450 μL DPBS/BSA buffer (Dulbecco's phosphate-buffered saline with 0.5% BSA) and 50 μL CD90.1 MicroBeads solution (130-121-273, Miltenyi Biotec) was added. The cell suspension was mixed, incubated, and centrifuged before the positive selection of RGCs using magnetic separation. The retinal single-cell suspension containing RGCs was sequentially passed through two separate MS columns (130-042-201, Miltenyi Biotec) in the magnetic field of a MiniMACS Separation Unit (130-042-102, Miltenyi Biotec) to bind the RGCs in the column and wash other cell types out of the columns. The magnetically labeled RGCs were flushed from the first MS column to the second MS column for additional purification. RGCs were flushed from the second MS column with pre-warmed RGC growth medium (serum free, made according to the recipe of Winzeler and Wang [36]). Isolated RGCs were seeded on coated surfaces at a density of 2.00×10^4 cells per coverslip and grown for 5 days in a 37°C and 5% CO_2 incubator. Mechanical stimulation was applied to test cell adherence to the coatings on day 5 after isolation.

2.4 | Application of Mechanical Stimulation

In order to establish a reproducible and objective method of mechanical stimulation that would give information about the adherence of cells to different surfaces, we chose to use a thermomixer. The thermomixer (Eppendorf ThermoMixer C, 5382) was set to shake at 500RPM for 1 min at 37°C. Cells were fixed immediately after mechanical stimulation or returned to the incubator (at 37°C and 5% CO_2) for 24 h.

2.5 | Staining and Imaging of Cell Density and Cell Death

Primary RGCs and PC-12 cells were treated similarly for staining and imaging. Cells were fixed with 4% paraformaldehyde (PFA) (Sigma-Aldrich) in PBS at room temperature for 30 min immediately after mechanical stimulation or 24 h after mechanical stimulation; at the same time points, corresponding unstimulated controls were fixed as well (images shown in the results section are all 24 h after mechanical stimulation or their controls). For immunocytochemistry, cells were permeabilised with 0.1% Triton X-100 (Merck) in PBS at room temperature for 15 min and blocked with 1% BSA (VWR) in PBS for 1 h at room temperature. Neuronal cells and their axons were stained using chicken anti-β-III-tubulin antibody (1:1000; NB100-1612, Novus Biologicals) incubated overnight at 4°C. Alexa Fluor 647 goat anti-chicken (1:500, A-21449, Thermo Fisher) was used as secondary antibody, incubated at room temperature for 1 h. All antibody solutions contained 0.2% BSA and 0.1% Triton X-100. Cell death was detected using a TUNEL technology with a Fluorescein In Situ Cell Death Detection Kit (11,684,795,910, Roche). The working solution was prepared according to the manufacturer's protocol and 50 μL per coverslip or 100 μL per well of this solution was incubated for 1 h at 37°C. Nuclei of cells were stained using 4′,6-diamidino-2-phenylindole dihydrochloride (DAPI; 32,670, Sigma-Aldrich) at room temperature for 10 min. All samples were imaged with an automated inverted Nikon Ti-E microscope, equipped with a Lumencor Spectra light source, an Andor Zyla 5.5 sCMOS camera, and an MCL NANO Z200-N TI z-stage. Excitation wavelengths 390 nm, 480 nm, and 647 nm were used in combination with emission filters DAPI, FITC, and Cy5. Imaging was performed with 10× and 20× objectives (CFI PLAN APO LBDA 10X 0.45/4 mm and CFI Plan Apochromat K 20X NA 0.75 WD 1). Five to 10 semi-random fields of view (dispersed evenly over the culture area, including the center and periphery of the coverslip or well) were captured in both magnifications and three wavelengths (390, 480, and 647 nm). A magnification of 10× was used to get an overview of the coverslip (cell distribution and general morphology) whereas 20× was used to quantify cell density and cell death and to assess morphology in more detail.

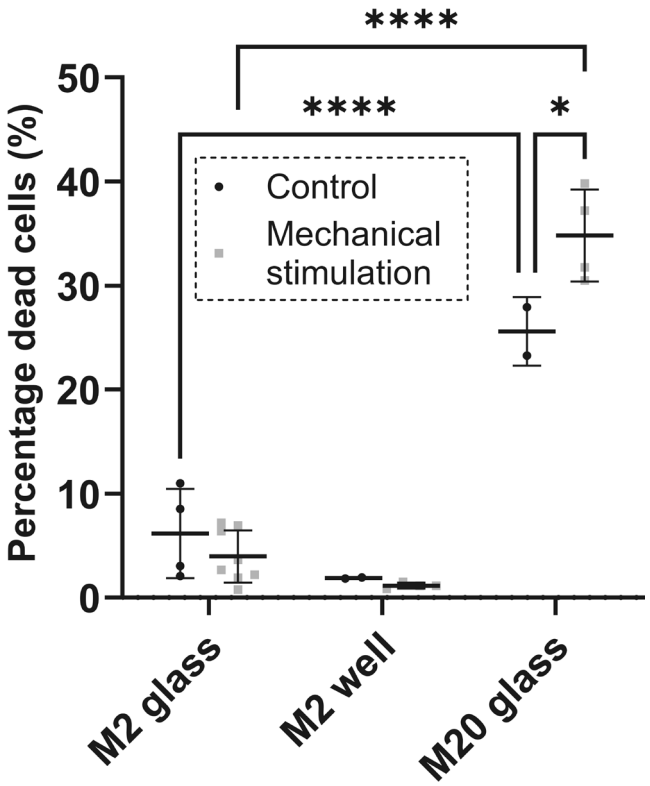

FIGURE 1 | Percentage of TUNEL+ to DAPI+ cells as a measure of cell death of PC12 cells, cultured on glass coverslips and tissue culture plastic wells with M2 and M20 coating. The data points indicated in the figure represent the mean values of each coverslip based on measuring 5–10 random fields of view per coverslip. Cell death staining of the M20 well was not performed.

2.6 | Image Analysis

Quantification of cell density and cell death was performed using the "Find Maxima..." process with prominence = 400 in ImageJ (FIJI) [54]. Counts were corrected manually to exclude false positives (e.g., debris) and include false negatives (e.g., low intensity, cells in clusters). NIS Elements Viewer (5.21.00, Laboratory Imaging) was used to view

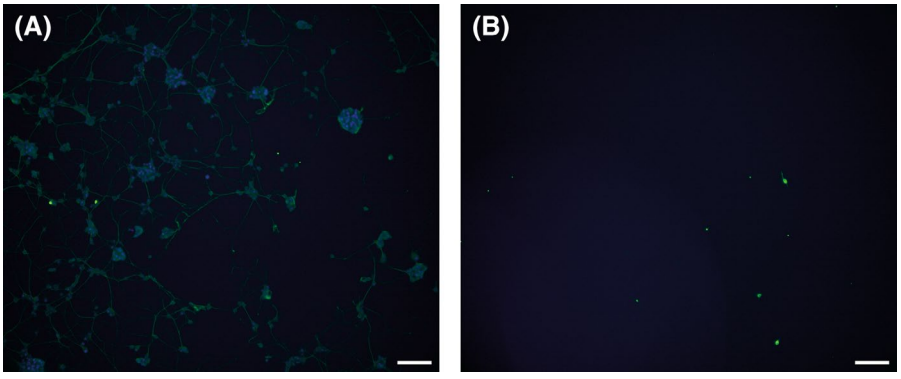

FIGURE 2 | (A) Representative image of PC-12 cells cultured on a S20 coated well in the control condition presenting a large number of cells with elaborate neurites and some empty regions. (B) Representative image of PC-12 cells cultured on a S20 coated well 24 h after mechanical stimulation showing very few cells remaining. Scale bar = 100 μm, blue = DAPI, green = β-III-tubulin.

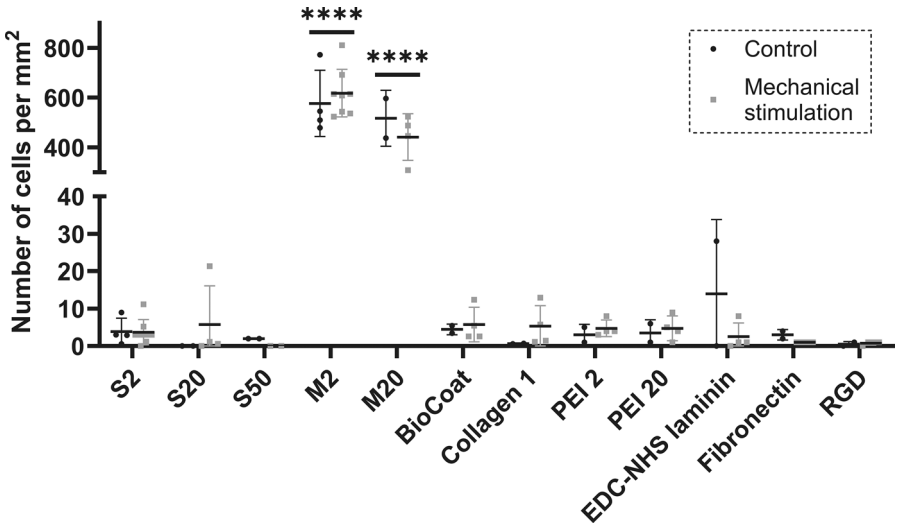

FIGURE 3 | PC-12 cell density (cells per mm^2) on glass coverslips with different coatings. ****: Both M2 and M20 have a higher density than the other coating strategies in the corresponding conditions (control and mechanical stimulation, all $p < 0.0001$). M2 versus M20 is significantly different in the mechanical stimulation condition (p-value 0.002). No significant difference was found between control and mechanical stimulation conditions within each coating. The data points indicated in the figure represent the mean values of each coverslip based on measuring 5–10 random fields of view per coverslip.

segmentation and assess morphology and neurite outgrowth qualitatively.

Neurite length was calculated using ImageJ (FIJI) [54] macros. Images stained with anti-β-III-tubulin were converted to a mask using "setThreshold..." and Skeletonized. Cell bodies were subtracted from the skeletonized image, and the area of neurites was calculated using "Analyze Particles...." Since the skeletonized neurites are 1 pixel wide, the area of neurites is equal to the total length of the neurites (in pixels). Average neurite length was calculated by dividing the total neurite length by the number of cells (as described above).

2.7 | Statistical Analysis and Graphical Representation

All cells in five to 10 random fields of view were counted, and mean values were calculated per coverslip. Each coverslip yields one data point and is represented as the number of replicates (n). All mean values were graphically plotted and statistically tested with a Two-way ANOVA with Tukey multiple comparisons test correction using GraphPad Prism (Version 10.2.2). p-values: * < 0.05, ** < 0.01, *** < 0.001, **** < 0.0001.

3 | Results

The aim of the present study was to find a coated surface that allows retinal ganglion cells (RGCs) to adhere and grow well and remain attached both under normal conditions and under mechanical stimulation. A wide range of surfaces and coatings was first screened with the rat pheochromocytoma cell line (PC-12) as a model for neuronal cells. Next, a small selection of these coatings was tested with primary rat RGCs.

3.1 | Glass Surface Preparation With Ethanol or Piranha Solution

First, we compared two methods of cleaning and preparing the glass surfaces. Twelve millimeter glass coverslips were chosen as a baseline surface, as they are widely used in literature [20, 21, 36–38, 55, 56]. The first method consisted of washing coverslips with ethanol for more than 1 month to provide a clean coating surface according to the protocol of Winzeler & Wang [36]. The second surface treatment technique was etching coverslips with Piranha solution [49]. Prepared surfaces were coated in two ways (S50: sequential coating with 10 µg/mL PDL and then 50 µg/mL laminin, or M20: mixed coating with 10 µg/mL PDL and 20 µg/mL laminin) to assess which method would work best for culturing neuronal cells. Both surface preparation techniques gave similar results in cell density and morphology (mean cell density of PC-12 cells cultured on ethanol treated M20 coated glass coverslips was 142.5, compared to 142.1 on piranha-etched M20 coated coverslips, seeded at a density of 2.00×10^4 cells per coverslip). The rest of the study was performed only with piranha-etched coverslips, as this technique assured a consistent supply of clean glass coverslips with minimal time investment.

3.2 | Comparing Glass and Plastic Surfaces

Next, Ibidi polymer coverslips were compared to glass as a coating surface. Uncoated Ibidi polymer coverslips were manually punched to 12 mm coverslips, coated with M20, and compared to M20 coated glass coverslips. We noticed that the polymer coverslips often started floating on top of the cell culture medium, which caused drying of the cells. This made the polymer coverslips unsuitable for this test.

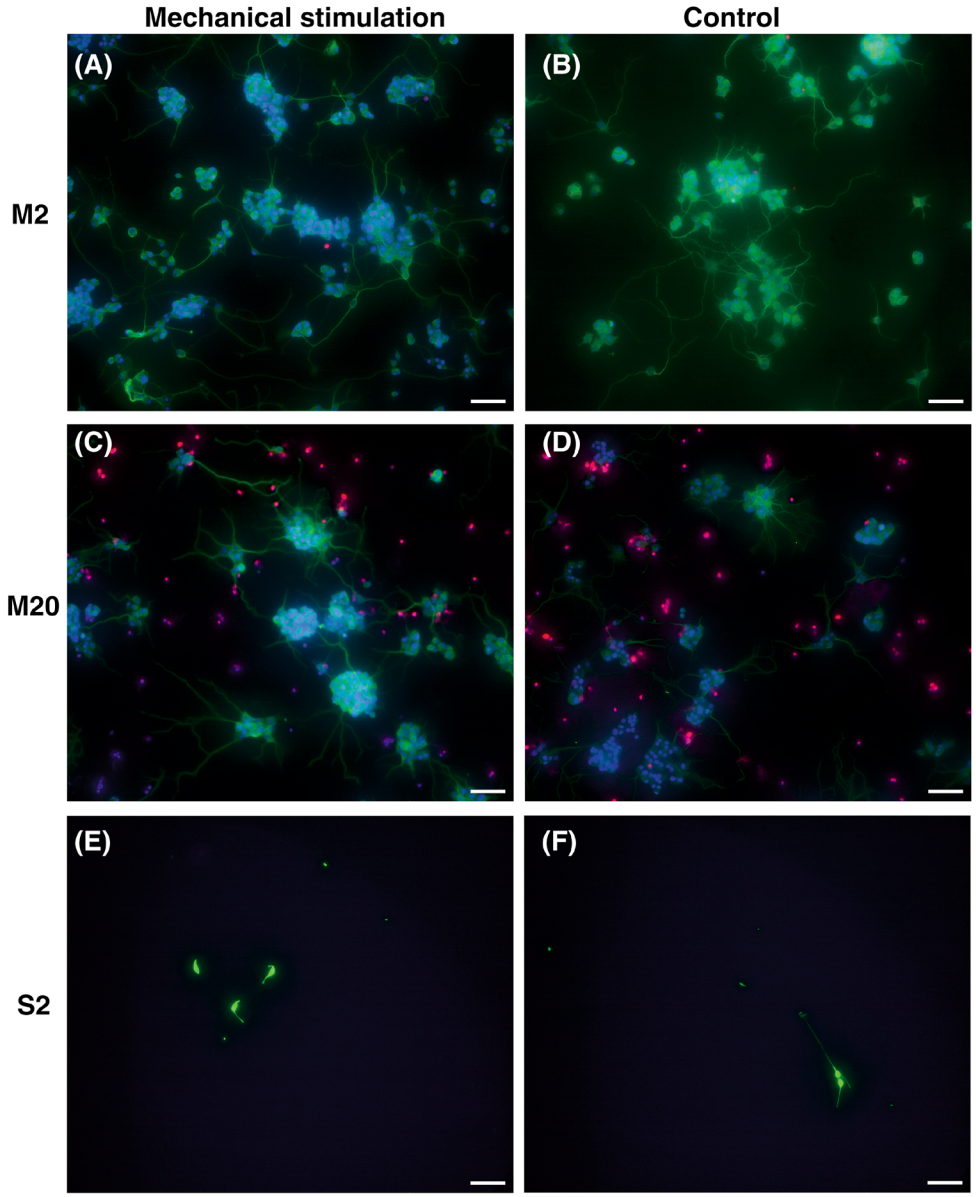

FIGURE 4 | Representative images of PC-12 cells cultured on PDL/laminin coated glass coverslips. (A, B): 2 μg/mL mixed protocol (M2). (C, D): 20 μg/mL mixed protocol (M20). (E, F): 2 μg/mL sequential coating (S2). Images of control condition are shown in (A, C, E). Images fixed and stained 24 h after mechanical stimulation are shown in (B, D, F). Scale bar = 100 μm, blue = DAPI, green = β-III-tubulin, red = TUNEL.

As an alternative polymer surface, we tested untreated 24-well plate tissue culture plastic. A selection of coatings and coating concentrations was tested on this surface, that is, S2 (sequential coating with 10 μg/mL PDL and then 2 μg/mL laminin), S20 (sequential coating with 10 μg/mL PDL and then 20 μg/mL laminin), Collagen 1, M2 (mixed coating with 10 μg/mL PDL and 2 μg/mL laminin), and M20. We did not observe significant differences between the number of cells on glass versus tissue culture plastic wells. Yet, quantification of cell death showed a higher percentage of dead cells on M20 coating compared to M2 coating ($p < 0.0001$ in both control and mechanical stimulation on glass coverslips, Figure 1). Cell death was significantly higher in the mechanical stimulation condition on M20 coated glass compared to control ($p = 0.0276$). No cell death differences were found between the two surfaces and two conditions with M2 coating. Cell death staining of wells with M20 coating was not performed.

In addition, we observed that the wells often showed areas without cells, both in the control (empty regions) and in the mechanical stimulation condition (almost no cells present; Figure 2). For microscopy purposes, glass coverslips are more convenient, and therefore we preferred this substrate for the experiments with RGCs.

Overall, considering both cell density and cell death, M2 coating on glass coverslips appeared to provide a favorable substrate for PC-12 cells.

3.3 | Comparing Coatings With PC-12 Cells

Continuing with piranha-etched glass coverslips, we tested various coatings. Figure 3 shows PC-12 cell density on the studied coatings. A clearly higher cell density was observed in mixed

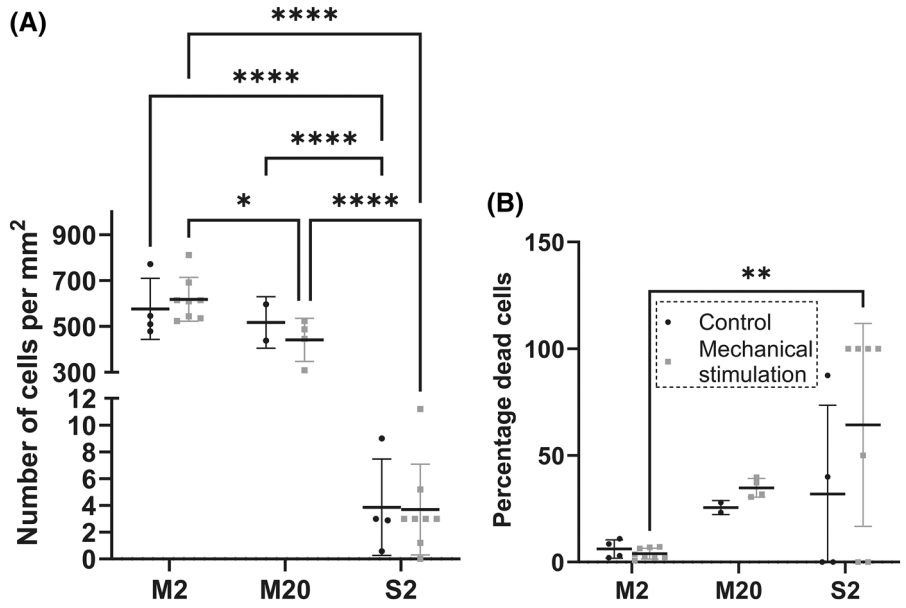

FIGURE 5 | (A) PC-12 cell density (cells per millimeter square) cultured on glass coverslips with different coatings. (B) Percentage of TUNEL+ to DAPI+ cells as a measure of cell death. ****: Both control and Mechanical stimulation in S2 are significantly different from the corresponding conditions in M2 and M20 ($p < 0.0001$). *: M2 versusM20 are significantly different in the mechanical stimulation condition (p-value 0.017). No significant difference in the control condition of M2 versus M20. A significant difference was found in cell death between mechanical stimulation conditions of M2 versus S2 (**p-value 0.0057). No difference was found within each coating. The data points indicated in the figure represent the mean values of each coverslip based on measuring 5–10 random fields of view per coverslip.

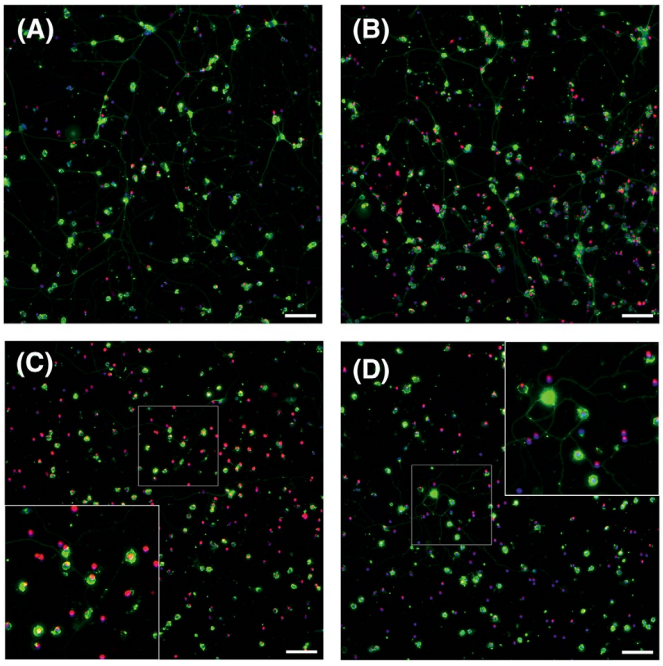

FIGURE 6 | Representative images of RGCs cultured on PDL/laminin coated glass coverslips. (A, B): 2 μg/mL sequential coating (S2). (C, D): 2 μg/mL mixed protocol (M2). Images of control condition are shown in (A, C). Images fixed and stained 24 h after mechanical stimulation are shown in (B, D). Scale bar = 100 μm, blue = DAPI, green = β-III-tubulin, red = TUNEL, insets show higher magnification of indicated area (white box).

PDL/laminin coatings (M2 and M20) compared to the other coating strategies ($p < 0.0001$). Furthermore, M2 had a significantly higher cell density compared to M20 in the mechanical stimulation condition ($p = 0.002$). For all tested coatings, we found no significant differences between the control condition and mechanical stimulation condition, with our settings of mechanical stimulation.

Apart from the mixed PDL/laminin coatings (M2 and M20), the different coating strategies showed very low cell density (Figure 3). Sequential PDL/laminin coatings showed very low cell densities in S2 (2 μg/mL laminin), S20 (20 μg/mL), and S50 (50 μg/mL), making it a poor coating strategy for PC-12 cells. The same accounted for BioCoat, Collagen 1, PEI 2, PEI 20, EDC-NHS laminin, Fibronectin, and RGD.

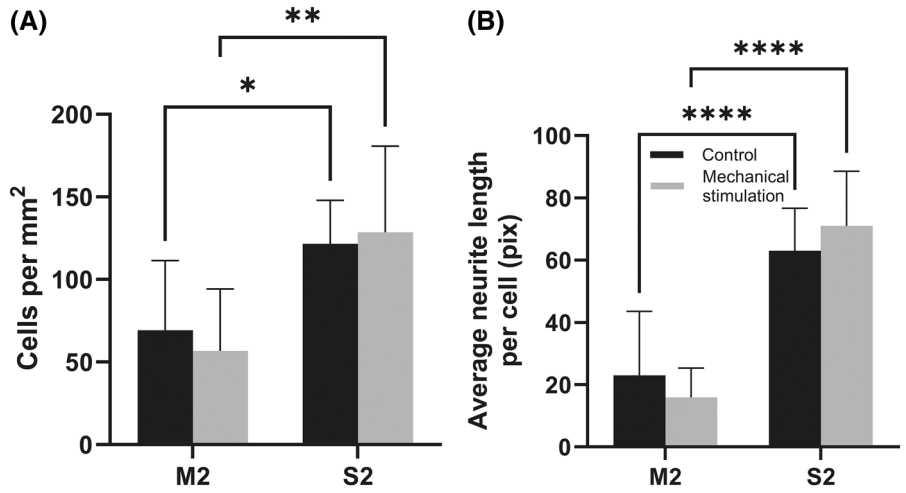

FIGURE 7 | (A) Cell density of RGCs (per millimeter square). A significant difference in cell density was found between M2 and S2 coating in both the control condition (*$p = 0.0365$) and mechanical stimulation condition (**$p = 0.0056$). No difference was found within each coating. $n = 9$–10 for control, $n = 8$ for mechanical stimulation. (B) A significant difference in average neurite length per cell (in pixels) was found between M2 and S2 coating in both the control and mechanical stimulation condition. No significant difference was found within each condition (***$p \leq 0.0001$). $n = 10$ for S2 control, $n = 9$ for M2 control, $n = 8$ for both S2 and M2 mechanical stimulation. Each replicate represents the mean values of each coverslip based on measuring 5–10 random fields of view per coverslip.

For the best scoring coatings (mixed PDL/laminin, M2 and M20), cell death was assessed and compared with cell death on the coating used mostly for RGCs, which is a sequential coating of PDL and 2 μg/mL laminin (S2) [16, 19, 36]. Figure 4 portrays representative images of the various PDL/laminin coated coverslips. Morphological assessment of PC-12 cells on these coatings showed large differences in cell density, with S2 having the lowest cell density (Figure 5). High cell density and elaborate neurite networks were present on both laminin concentrations of the mixed PDL/laminin coatings (in the control as well as the mechanical stimulation condition). M20 (20 μg/mL) had more and larger cell clusters. In addition, there were more dead cells in the higher laminin concentration coating.

The effect of these coatings on cell death is shown in Figure 5B, whereas Figure 5A shows the cell density of these coatings for comparison to cell death. A significant difference in cell density between the S2 coating and the other coatings was observed in both the control and mechanical stimulation conditions (Figure 5A; $p < 0.0001$). Mixed coating with 2 μg/mL laminin (M2) showed the lowest cell death and sequential coating showed the highest cell death, highlighting again that sequential PDL/laminin coatings are unsuitable for PC-12 cells (Figure 5B). The high variability in the results of S2 is probably related to the very low number of cells remaining on this coating. In summary, considering cell density and cell death percentage in both control and mechanical strain conditions, the M2 coating appeared best for PC-12 cells.

TABLE 1 | Summary of results.

Coating	PC-12 cells	RGCs
Sequential PDL/laminin 2 μg/mL (S2)	Low density	High density, elaborate neurites
Sequential PDL/laminin 20 μg/mL (S20)	Low density	—
Sequential PDL/laminin 50 μg/mL (S50)	Low density	—
Mixed PDL/laminin 2 μg/mL (M2)	High density, low cell death, elaborate neurites	High density, few cells with neurites
Mixed PDL/laminin 20 μg/mL (M20)	High density, high cell death, elaborate neurites	—
BioCoat (PDL/laminin)	Low density	—
Collagen 1	Low density	—
PEI/laminin 2 μg/mL (PEI 2)	Low density	—
PEI/laminin 20 μg/mL (PEI 20)	Low density	—
EDC-NHS laminin	Low density	—
Fibronectin	Low density	—
RGD	Low density	—

3.4 | Comparing Coatings With RGCs

Next, the coating that performed best with PC-12 cells in terms of cell density and cell death was studied with the primary RGCs, that is, M2 coating (mixed PDL/laminin coating with 2 μg/mL laminin). This coating was compared to the coating mostly used for primary RGCs, that is, S2 coating (sequential coating of PDL and 2 μg/mL laminin) [16, 19, 36]. Cell density, cell death, and morphology of primary RGCs were measured.

Morphological assessment showed a marked difference between the two coatings studied with RGCs (Figure 6). There was a distinct difference in RGC morphology. RGCs on the sequential coating (S2) exhibited a large network of neurites, whereas RGCs on the mixed coating (M2) were less elaborate in neurite growth, both in terms of complexity and in percentage of cells with neurites. There were no visible differences in morphology between the control and mechanical stimulation conditions for both coatings. DAPI-positive but β-III-tubulin-negative cells were shown to be TUNEL positive and therefore dead cells (as shown in Figures 4 and 6 in red).

We noticed that the isolation of primary rat RGCs caused a considerable amount of cell death of these cells. When calculating cell density, we took care to count only the healthy, living cells, which showed no TUNEL signal and normal neuronal cell morphology. Cell density showed a significant difference between the two coatings. Sequential coating (S2) had a significantly higher density than mixed coating (M2) in both the control ($p = 0.0365$) and mechanical stimulation ($p = 0.0056$) conditions (Figure 7A). For each coating, there was no significant difference in density between the control and mechanical stimulation conditions.

Additional analysis showed that the coating composition influences neurite length as well. Average neurite length per cell was significantly larger in RGC cultured on S2 coating compared to M2 in both control and mechanical strain conditions (Figure 7B; $p < 0.0001$). There were no statistically significant differences between the control and mechanical stimulation conditions for both coatings.

In summary, combining criteria of cell density, morphology, and neurite length, the S2 coating appeared superior to the M2 coating for RGCs.

4 | Discussion and Conclusion

We tested various coatings and coating protocols, aiming to find an optimal substrate for adherence and growth of PC-12 cells and retinal ganglion cells (RGCs) in control conditions as well as conditions of mechanical strain. Most tested coatings did not provide a suitable substrate for PC-12 cells. The best PC-12 cell density was achieved with a coating of PDL mixed with 2 μg/mL laminin in PBS (M2). In comparison to PC-12 cells, RGCs appeared to prefer sequential PDL/laminin coating (S2): This sequential coating protocol was more favorable for both cell density and morphology of RGCs. A summary of the results is presented in Table 1.

While RGCs are the most relevant cells for glaucoma, we used the neuronal cell line PC-12 for initial screening of coatings in order to reduce the use of animals and to have a reliable source of cells for medium-throughput screening of surfaces and coatings. The PC-12 neuronal cell line shows elaborate neurite outgrowth, is easy to expand, and is of rat origin. In addition, PC-12 cells are commonly used as a model for neuronal cells, and more specifically, for RGCs [34, 35, 57, 58].

We tested two methods of preparing and cleaning the glass surface before applying the coating. Cleaning with ethanol [59] or Piranha etching [49, 60] did not result in clear differences in PC-12 cell culture.

Comparing glass and plastic surfaces, we noticed that glass was superior for culturing PC-12 cells, particularly using the M2 coating. The lower concentration of laminin may increase the availability of PDL for PC-12 cells.

Many coating strategies resulted in a low number of cells that remained attached after a few days of culturing both with and without mechanical stimulation. Most of these strategies already showed low cell densities in the control condition. This suggests these coatings did not facilitate sufficient attachment for the cells or did not hold the cells enough to withstand the small forces exerted during medium changes, fixation, and staining procedures, despite careful and standardized manipulation. Results depicted in Figure 2 indicate that the latter may indeed play a role since empty regions were found where cells appeared to be washed off the coverslips. Most coating strategies that contained very few to no cells were not assessed for cell death, since the very low cell density already disqualified them.

Results of this study indicate that not only the coating composition influences cell attachment, but the protocol of coating appears to be important as well. Mixed PDL/laminin coatings yielded the largest cell density for PC-12 cells, while a lower laminin concentration (2 μg/mL, M2) seemed to outperform higher laminin concentrations in terms of cell death. The best performing coating in PC-12 cells (mixed PDL/laminin 2 μg/mL, M2) also provided a good surface for RGCs in terms of cell density. In contrast, with regard to RGCs, the most commonly utilized coating, sequential PDL/laminin 2 μg/mL (S2), yielded superior results: an increased cell density and notably enhanced RGC morphology, characterized by greater neurite growth and neurite complexity on S2 coating. Note that cell density is one of the factors that can influence RGC survival [61]. Here we used a high density.

If we look at the extracellular matrix (ECM) composition of the retina, it seems logical that laminin is the preferred substrate for primary RGC cultures as laminins are present in the native tissue. Laminins in the retina have been found in the ganglion cell layer (GCL) around RGCs and in the internal limiting membrane. They are involved in RGC migration and development [19, 39, 50, 62–66]. There are different types of laminins, such as Laminin-111 (also known as laminin 1 produced by Engelbreth-Holm-Swarm (EHS) sarcoma) used in this study, which is commonly used in neural cultures and has been found to be important for optic cup and retinal development and for RGC axonal growth [67, 68]. Laminins, like other ECM proteins, interact with integrin receptors of cells. Integrin signaling is a key component for mechanotransduction [69]. Each combination of α and β integrin subunits has distinct properties and often recognizes several ECM proteins; individual ECM proteins bind to various integrins [66]. RGCs use laminin as an extracellular signal for migration, lamination, and axonal orientation [70, 71]. Riccomagno et al. [72] have shown that RGCs interact with laminin through the β1-integrin subunit and their immunohistochemical analyses indicate that β1-Integrin is involved in GCL migration and organization. Other integrin subunits found in the GCL are α1, α3, α5, αV, β1, and β3, while RGCs

cultured on laminin did not express αV [66]. Vecino et al. [66] suggest RGCs either use α3β1 or α5β1 to adhere to laminin and that integrin α5β1 is more likely involved in RGC growth on laminin than α3β1. Apart from laminin, adult RGCs are in vivo also in contact with collagen I, collagen IV, and fibronectin [66]. PC-12 cells were found to mainly use integrin α1β1 and α3β1 to interact with laminin, while only α1β1 is used for collagen types I and IV [73]. Integrin α5 expression in PC-12 cells is very low [74]. This difference in integrin expression between PC-12 cells and RGCs may contribute to neurite growth and survival differences that we have observed between sequential and mixed PDL/laminin coatings. The exact explanation is however unknown. The availability of PDL to the cells is probably another important factor. In sequential coatings, laminin may fully cover the PDL surface, while the mixed coating would also provide cell contact with PDL. PDL is used to couple laminin to glass coverslips since both laminin as well as glass coverslips are negatively charged. The positively charged PDL facilitates laminin binding to the glass coverslip. Wysotzki et al. [9] suggested a possible additional effect of layer-by-layer PDL laminin coating, that is, a polarization of the laminin molecule inducing a positive charge on the side where cells interact with the coating. We could speculate that RGCs benefit more from the polarization of laminin, particularly for neurite growth and cell survival. The absence of certain integrins in PC-12 cells may explain why these cells need PDL in closer proximity to the cell in order to firmly adhere. Other factors such as substrate stiffness and topographical cues are possibly contributing together with ECM composition, as shown in PC-12 cells [75, 76]. This was however beyond the scope of this paper.

Regarding mechanical stimulation, our experiments were less conclusive. While we observed that our mechanical stimulus increased the percentage of dead cells in the PC-12 cell cultures, we did not find a significant effect on RGCs. In our ongoing research, we currently explore other mechanical triggers, more relevant for glaucoma, to characterize the behavior of RGCs under mechanical stimulation.

In conclusion, different coatings resulted in large differences in cell densities after seeding PC-12 cells. Mixed coatings of PDL and laminin (M2 and M20) worked best for adherence and growth of PC-12. When comparing with primary rat RGCs, we noticed cell type dependent differences with respect to cell morphology and cell death: Sequential coating of PDL and laminin (S2) was best for adherence, neurite growth, and cell survival for RGCs (Table 1). We conclude that the optimal coating depends on the cell type. When reporting cell culture studies, it is important to fully specify culture surface, surface treatment, and coating protocol, since all these factors influence cell attachment, growth, and survival [77].

Acknowledgments

We thank Jeroen Rouwkema, Ravi Sinha, Denis van Beurden, Urandelger Tuvshindorj, and Rebeca Rivero for their help in conceptualizing and helping with coverslip preparation. We thank the following foundations for their support coordinated by UitZicht: Glaucoomfonds, Oogfonds, Landelijke Stichting voor Blinden en Slechtzienden (LSBS), and Rotterdamse Stichting Blindenbelangen. The funders had no role in study design, analysis, decision to publish, or preparation of the manuscript.

Conflicts of Interest

The authors declare no conflicts of interest.

Data Availability Statement

The data that support the findings of this study are available from the corresponding author upon reasonable request.

References

1. P. N. Sergi and E. A. Cavalcanti-Adam, "Biomaterials and Computation: A Strategic Alliance to Investigate Emergent Responses of Neural Cells," *Biomaterials Science* 5 (2017): 648–657, https://doi.org/10.1039/c6bm00871b.

2. B. Geiger, J. P. Spatz, and A. D. Bershadsky, "Environmental Sensing Through Focal Adhesions," *Nature Reviews. Molecular Cell Biology* 10 (2009): 21–33, https://doi.org/10.1038/nrm2593.

3. P. A. Janmey, D. A. Fletcher, and C. A. Reinhart-King, "Stiffness Sensing by Cells," *Physiological Reviews* 100 (2020): 695–724, https://doi.org/10.1152/physrev.00013.2019.

4. J. E. Meredith, Jr., B. Fazeli, and M. A. Schwartz, "The Extracellular Matrix as a Cell Survival Factor," *Molecular Biology of the Cell* 4 (1993): 953–961, https://doi.org/10.1091/mbc.4.9.953.

5. J. E. Murphy-Ullrich, "Thrombospondin-1 Signaling Through the Calreticulin/LDL Receptor Related Protein 1 Axis: Functions and Possible Roles in Glaucoma," *Frontiers in Cell and Development Biology* 10 (2022): 898772, https://doi.org/10.3389/fcell.2022.898772.

6. Y. Maekawa, A. Onishi, K. Matsushita, et al., "Optimized Culture System to Induce Neurite Outgrowth From Retinal Ganglion Cells in Three-Dimensional Retinal Aggregates Differentiated From Mouse and Human Embryonic Stem Cells," *Current Eye Research* 41, no. 4 (2016): 558–568, https://doi.org/10.3109/02713683.2015.1038359.

7. Y. Sun, Z. Huang, W. Liu, et al., "Surface Coating as a Key Parameter in Engineering Neuronal Network Structures In Vitro," *Biointerphases* 7 (2012): 29, https://doi.org/10.1007/s13758-012-0029-7.

8. H. Ai, H. Meng, I. Ichinose, et al., "Biocompatibility of Layer-By-Layer Self-Assembled Nanofilm on Silicone Rubber for Neurons," *Journal of Neuroscience Methods* 128 (2003): 1–8, https://doi.org/10.1016/s0165-0270(03)00191-2.

9. P. Wysotzki and J. Gimsa, "Surface Coatings Modulate the Differences in the Adhesion Forces of Eukaryotic and Prokaryotic Cells as Detected by Single Cell Force Microscopy," *International Journal of Biomaterials* 2019 (2019): 7024259, https://doi.org/10.1155/2019/7024259.

10. R. A. Fischer, Y. Zhang, M. L. Risner, D. Li, Y. Xu, and R. M. Sappington, "Impact of Graphene on the Efficacy of Neuron Culture Substrates," *Advanced Healthcare Materials* 7 (2018): e1701290, https://doi.org/10.1002/adhm.201701290.

11. A. Blau, C. Weinl, J. Mack, S. Kienle, G. Jung, and C. Ziegler, "Promotion of Neural Cell Adhesion by Electrochemically Generated and Functionalized Polymer Films," *Journal of Neuroscience Methods* 112 (2001): 65–73, https://doi.org/10.1016/s0165-0270(01)00458-7.

12. D. Krizaj, D. A. Ryskamp, N. Tian, et al., "From Mechanosensitivity to Inflammatory Responses: New Players in the Pathology of Glaucoma," *Current Eye Research* 39 (2014): 105–119, https://doi.org/10.3109/02713683.2013.836541.

13. D. Krizaj, *Webvision: The Organization of the Retina and Visual System*, ed. H. Kolb, E. Fernandez, and R. Nelson (Webvision, 1995).

14. P. Vroemen, T. Gorgels, C. A. B. Webers, and J. de Boer, "Modeling the Mechanical Parameters of Glaucoma," *Tissue Engineering. Part B, Reviews* 25, no. 5 (2019): 412–428, https://doi.org/10.1089/ten.TEB.2019.0044.

15. D. S. Welsbie, K. L. Mitchell, V. Jaskula-Ranga, et al., "Enhanced Functional Genomic Screening Identifies Novel Mediators of Dual Leucine Zipper Kinase-Dependent Injury Signaling in Neurons," *Neuron* 94 (2017): 1142–1154, https://doi.org/10.1016/j.neuron.2017.06.008.

16. F. Gao, T. Li, J. Hu, X. Zhou, J. Wu, and Q. Wu, "Comparative Analysis of Three Purification Protocols for Retinal Ganglion Cells From Rat," *Molecular Vision* 22 (2016): 387–400.

17. W. Kobayashi, A. Onishi, H. Y. Tu, et al., "Culture Systems of Dissociated Mouse and Human Pluripotent Stem Cell-Derived Retinal Ganglion Cells Purified by Two-Step Immunopanning," *Investigative Ophthalmology & Visual Science* 59 (2018): 776–787, https://doi.org/10.1167/iovs.17-22406.

18. Y. H. Park, J. D. Snook, I. Zhuang, G. Shen, and B. J. Frankfort, "Optimized Culture of Retinal Ganglion Cells and Amacrine Cells From Adult Mice," *PLoS One* 15 (2020): e0242426, https://doi.org/10.1371/journal.pone.0242426.

19. K. E. Kador, R. B. Montero, P. Venugopalan, et al., "Tissue Engineering the Retinal Ganglion Cell Nerve Fiber Layer," *Biomaterials* 34 (2013): 4242–4250, https://doi.org/10.1016/j.biomaterials.2013.02.027.

20. P. Teotia, M. J. Van Hook, and I. Ahmad, "A co-Culture Model for Determining the Target Specificity of the De Novo Generated Retinal Ganglion Cells," *Bio-Protocol* 7, no. 7 (2017): e2212, https://doi.org/10.21769/BioProtoc.2212.

21. P. Sodhi and A. T. Hartwick, "Adenosine Modulates Light Responses of Rat Retinal Ganglion Cell Photoreceptors Througha cAMP-Mediated Pathway," *Journal of Physiology* 592, no. 19 (2014): 4201–4220, https://doi.org/10.1113/jphysiol.2014.276220.

22. K. E. Kador, S. P. Grogan, E. W. Dorthé, et al., "Control of Retinal Ganglion Cell Positioning and Neurite Growth: Combining 3D Printing With Radial Electrospun Scaffolds," *Tissue Engineering. Part A* 22 (2016): 286–294, https://doi.org/10.1089/ten.TEA.2015.0373.

23. K. C. Chang, M. Bian, X. Xia, et al., "Posttranslational Modification of Sox11 Regulates RGC Survival and Axon Regeneration," *eNeuro* 8, no. 1 (2021): ENEURO.0358-20.2020, https://doi.org/10.1523/ENEURO.0358-20.2020.

24. N. Ruzafa, X. Pereiro, A. Fonollosa, J. Araiz, A. Acera, and E. Vecino, "Plasma Rich in Growth Factors (PRGF) Increases the Number of Retinal Müller Glia in Culture but Not the Survival of Retinal Neurons," *Frontiers in Pharmacology* 12 (2021): 606275, https://doi.org/10.3389/fphar.2021.606275.

25. H. Takeuchi, S. Inagaki, W. Morozumi, et al., "VGF Nerve Growth Factor Inducible Is Involved in Retinal Ganglion Cells Death Induced by Optic Nerve Crush," *Scientific Reports* 8 (2018): 16443, https://doi.org/10.1038/s41598-018-34585-3.

26. Y. Iwata, S. Inagaki, W. Morozumi, S. Nakamura, H. Hara, and M. Shimazawa, "Treatment With GDF15, a TGFbeta Superfamily Protein, Induces Protective Effect on Retinal Ganglion Cells," *Experimental Eye Research* 202 (2021): 108338, https://doi.org/10.1016/j.exer.2020.108338.

27. Y. Y. Fang, M. Luo, S. Yue, et al., "7,8-Dihydroxyflavone Protects Retinal Ganglion Cells Against Chronic Intermittent Hypoxia-Induced Oxidative Stress Damage via Activation of the BDNF/TrkB Signaling Pathway," *Sleep & Breathing* 26 (2022): 287–295, https://doi.org/10.1007/s11325-021-02400-5.

28. R. Boia, P. A. N. Dias, C. Galindo-Romero, et al., "Intraocular Implants Loaded With A3R Agonist Rescue Retinal Ganglion Cells From Ischemic Damage," *Journal of Controlled Release* 343 (2022): 469–481, https://doi.org/10.1016/j.jconrel.2022.02.001.

29. J. Zhao, G. B. Gonsalvez, B. A. Mysona, S. B. Smith, and K. E. Bollinger, "Sigma 1 Receptor Contributes to Astrocyte-Mediated Retinal Ganglion Cell Protection," *Investigative Ophthalmology & Visual Science* 63 (2022): 1, https://doi.org/10.1167/iovs.63.2.1.

30. J. Beros, J. Rodger, and A. R. Harvey, "Age Related Response of Neonatal Rat Retinal Ganglion Cells to Reduced TrkB Signaling In Vitro and In Vivo," *Frontiers in Cell and Development Biology* 9 (2021): 671087, https://doi.org/10.3389/fcell.2021.671087.

31. B. Mead, A. Kerr, N. Nakaya, and S. I. Tomarev, "miRNA Changes in Retinal Ganglion Cells After Optic Nerve Crush and Glaucomatous Damage," *Cells* 10 (2021): 1564, https://doi.org/10.3390/cells10071564.

32. W. Morozumi, S. Inagaki, Y. Iwata, S. Nakamura, H. Hara, and M. Shimazawa, "Piezo Channel Plays a Part in Retinal Ganglion Cell Damage," *Experimental Eye Research* 191 (2020): 107900, https://doi.org/10.1016/j.exer.2019.107900.

33. Y. Ge, R. Zhang, Y. Feng, and H. Li, "Mbd2 Mediates Retinal Cell Apoptosis by Targeting the lncRNA Mbd2-AL1/miR-188-3p/Traf3 Axis in Ischemia/Reperfusion Injury," *Molecular Therapy–Nucleic Acids* 19 (2020): 1250–1265, https://doi.org/10.1016/j.omtn.2020.01.011.

34. A. Agar, S. Li, N. Agarwal, M. T. Coroneo, and M. A. Hill, "Retinal Ganglion Cell Line Apoptosis Induced by Hydrostatic Pressure," *Brain Research* 1086 (2006): 191–200, https://doi.org/10.1016/j.brainres.2006.02.061.

35. L. Tok, M. Naziroglu, A. C. Uguz, and O. Tok, "Elevated Hydrostatic Pressures Induce Apoptosis and Oxidative Stress Through Mitochondrial Membrane Depolarization in PC12 Neuronal Cells: A Cell Culture Model of Glaucoma," *Journal of Receptor and Signal Transduction Research* 34 (2014): 410–416, https://doi.org/10.3109/10799893.2014.910812.

36. A. Winzeler and J. T. Wang, "Purification and Culture of Retinal Ganglion Cells From Rodents," *Cold Spring Harbor Protocols* 2013, no. 7 (2013): 643–652, https://doi.org/10.1101/pdb.prot074906.

37. E. M. Ullian, W. B. Barkis, S. Chen, J. S. Diamond, and B. A. Barres, "Invulnerability of Retinal Ganglion Cells to NMDA Excitotoxicity," *Molecular and Cellular Neurosciences* 26 (2004): 544–557, https://doi.org/10.1016/j.mcn.2004.05.002.

38. E. M. Ullian, B. T. Harris, A. Wu, J. R. Chan, and B. A. Barres, "Schwann Cells and Astrocytes Induce Synapse Formation by Spinal Motor Neurons in Culture," *Molecular and Cellular Neurosciences* 25 (2004): 241–251, https://doi.org/10.1016/j.mcn.2003.10.011.

39. F. Nafian, B. Kamali Doust Azad, S. Yazdani, M. J. Rasaee, and N. Daftarian, "A Lab-On-a-Chip Model of Glaucoma," *Brain and Behavior: A Cognitive Neuroscience Perspective* 10, no. 10 (2020): e01799, https://doi.org/10.1002/brb3.1799.

40. H. Teppola, J.-R. Sarkanen, T. O. Jalonen, and M.-L. Linne, "Impacts of Laminin and Polyethyleneimine Surface Coatings on Morphology of Differentiating Human SH-SY5Y Cells and Networks," in *European Medical and Biological Engineering Confernce* (Springer Singapore, 2017), 298–301.

41. S. A. Malin, B. M. Davis, and D. C. Molliver, "Production of Dissociated Sensory Neuron Cultures and Considerations for Their Use in Studying Neuronal Function and Plasticity," *Nature Protocols* 2 (2007): 152–160, https://doi.org/10.1038/nprot.2006.461.

42. A. Malheiro, F. Morgan, M. Baker, L. Moroni, and P. Wieringa, "A Three-Dimensional Biomimetic Peripheral Nerve Model for Drug Testing and Disease Modelling," *Biomaterials* 257 (2020): 120230, https://doi.org/10.1016/j.biomaterials.2020.120230.

43. X. Zhang, I. Mandric, K. H. Nguyen, et al., "Single Cell Transcriptomic Analyses Reveal the Impact of bHLH Factors on Human Retinal Organoid Development," *Frontiers in Cell and Development Biology* 9 (2021): 653305, https://doi.org/10.3389/fcell.2021.653305.

44. M. Rosario, R. Franke, C. Bednarski, and W. Birchmeier, "The Neurite Outgrowth Multiadaptor RhoGAP, NOMA-GAP, Regulates Neurite Extension Through SHP2 and Cdc42," *Journal of Cell Biology* 178 (2007): 503–516, https://doi.org/10.1083/jcb.200609146.

45. S. R. Farrell, I. D. Raymond, M. Foote, N. C. Brecha, and S. Barnes, "Modulation of Voltage-Gated Ion Channels in Rat Retinal Ganglion Cells Mediated by Somatostatin Receptor Subtype 4," *Journal of Neurophysiology* 104 (2010): 1347–1354, https://doi.org/10.1152/jn.00098.2010.

46. A. T. Hartwick, X. Zhang, B. C. Chauhan, and W. H. Baldridge, "Functional Assessment of Glutamate Clearance Mechanisms in a Chronic Rat Glaucoma Model Using Retinal Ganglion Cell Calcium Imaging," *Journal of Neurochemistry* 94, no. 3 (2005): 794–807, https://doi.org/10.1111/j.1471-4159.2005.03214.x.

47. R. Sinha, S. le Gac, N. Verdonschot, A. van den Berg, B. Koopman, and J. Rouwkema, "A Medium Throughput Device to Study the Effects of Combinations of Surface Strains and Fluid-Flow Shear Stresses on Cells," *Lab on a Chip* 15 (2015): 429–439, https://doi.org/10.1039/c4lc01259c.

48. D. F. Williams and J. M. Burke, "Modulation of Growth in Retina-Derived Cells by Extracellular Matrices," *Investigative Ophthalmology & Visual Science* 31 (1990): 1717–1723.

49. Z. Zhang, R. Yoo, M. Wells, T. P. Beebe, Jr., R. Biran, and P. Tresco, "Neurite Outgrowth on Well-Characterized Surfaces: Preparation and Characterization of Chemically and Spatially Controlled Fibronectin and RGD Substrates With Good Bioactivity," *Biomaterials* 26 (2005): 47–61, https://doi.org/10.1016/j.biomaterials.2004.02.004.

50. T. Wu, D. Li, Y. Wang, et al., "Laminin-Coated Nerve Guidance Conduits Based on Poly(l-Lactide-Co-Glycolide) Fibers and Yarns for Promoting Schwann Cells' Proliferation and Migration," *Journal of Materials Chemistry B* 5 (2017): 3186–3194, https://doi.org/10.1039/c6tb03330j.

51. U. Tuvshindorj, V. Trouillet, A. Vasilevich, et al., "The Galapagos Chip Platform for High-Throughput Screening of Cell Adhesive Chemical Micropatterns," *Small* 18 (2022): e2105704, https://doi.org/10.1002/smll.202105704.

52. S. D. Chandradoss, A. C. Haagsma, Y. K. Lee, J. H. Hwang, J. M. Nam, and C. Joo, "Surface Passivation for Single-Molecule Protein Studies," *Journal of Visualized Experiments* 24, no. 86 (2014): 50549, https://doi.org/10.3791/50549.

53. A. Winzeler and J. T. Wang, "Purification and Culture of Retinal Ganglion Cells," *Cold Spring Harbor Protocols* 2013, no. 7 (2013): 614–617, https://doi.org/10.1101/pdb.top070961.

54. J. Schindelin, I. Arganda-Carreras, E. Frise, et al., "Fiji: An Open-Source Platform for Biological-Image Analysis," *Nature Methods* 9 (2012): 676–682, https://doi.org/10.1038/nmeth.2019.

55. B. Castillo, Jr., M. del Cerro, X. O. Breakefield, et al., "Retinal Ganglion Cell Survival Is Promoted by Genetically Modified Astrocytes Designed to Secrete Brain-Derived Neurotrophic Factor (BDNF)," *Brain Research* 647 (1994): 30–36, https://doi.org/10.1016/0006-8993(94)91395-1.

56. B. A. Barres, B. E. Silverstein, D. P. Corey, and L. L. Chun, "Immunological, Morphological, and Electrophysiological Variation Among Retinal Ganglion Cells Purified by Panning," *Neuron* 1, no. 9 (1988): 791–803, https://doi.org/10.1016/0896-6273(88)90127-4.

57. A. Agar, S. S. Yip, M. A. Hill, and M. T. Coroneo, "Pressure Related Apoptosis in Neuronal Cell Lines," *Journal of Neuroscience Research* 60 (2000): 495–503, https://doi.org/10.1002/(SICI)1097-4547(20000515)60:4<495::AID-JNR8>3.0.CO;2-S.

58. R. R. Krishnamoorthy, A. F. Clark, D. Daudt, J. K. Vishwanatha, and T. Yorio, "A Forensic Path to RGC-5 Cell Line Identification: Lessons Learned," *Investigative Ophthalmology & Visual Science* 54 (2013): 5712–5719, https://doi.org/10.1167/iovs.13-12085.

59. B. A. Barres, "Designing and Troubleshooting Immunopanning Protocols for Purifying Neural Cells," *Cold Spring Harbor Protocols* 2014, no. 12 (2014): 1342–1347, https://doi.org/10.1101/pdb.ip073999.

60. B. F. Liu, J. Ma, Q. Y. Xu, and F. Z. Cui, "Regulation of Charged Groups and Laminin Patterns for Selective Neuronal Adhesion," *Colloids and Surfaces. B, Biointerfaces* 53 (2006): 175–178, https://doi.org/10.1016/j.colsurfb.2006.08.018.

61. A. Meyer-Franke, M. R. Kaplan, F. W. Pfrieger, and B. A. Barres, "Characterization of the Signaling Interactions That Promote the Survival and Growth of Developing Retinal Ganglion Cells in Culture," *Neuron* 15, no. 4 (1995): 805–819, https://doi.org/10.1016/0896-6273(95)90172-8.

62. R. T. Libby, M. F. Champliaud, T. Claudepierre, et al., "Laminin Expression in Adult and Developing Retinae: Evidence of Two Novel CNS Laminins," *Journal of Neuroscience* 20 (2000): 6517–6528.

63. K. Peynshaert, J. Devoldere, V. Forster, et al., "Toward Smart Design of Retinal Drug Carriers: A Novel Bovine Retinal Explant Model to Study the Barrier Role of the Vitreoretinal Interface," *Drug Delivery* 24 (2017): 1384–1394, https://doi.org/10.1080/10717544.2017.1375578.

64. S. K. Chintala, "The Emerging Role of Proteases in Retinal Ganglion Cell Death," *Experimental Eye Research* 82 (2006): 5–12, https://doi.org/10.1016/j.exer.2005.07.013.

65. A. R. Santos, R. G. Corredor, B. A. Obeso, et al., "β1 Integrin-Focal Adhesion Kinase (FAK) Signaling Modulates Retinal Ganglion Cell (RGC) Survival," *PLoS One* 7 (2012): e48332, https://doi.org/10.1371/journal.pone.0048332.

66. E. Vecino, J. P. Heller, P. Veiga-Crespo, K. R. Martin, and J. W. Fawcett, "Influence of Extracellular Matrix Components on the Expression of Integrins and Regeneration of Adult Retinal Ganglion Cells," *PLoS One* 10 (2015): e0125250, https://doi.org/10.1371/journal.pone.0125250.

67. N. Morissette and S. Carbonetto, "Laminin Alpha 2 Chain (M Chain) is Found Within the Pathway of Avian and Murine Retinal Projections," *Journal of Neuroscience* 15 (1995): 8067–8082.

68. B. Dorgau, M. Felemban, A. Sharpe, et al., "Laminin γ3 Plays an Important Role in Retinal Lamination, Photoreceptor Organisation and Ganglion Cell Differentiation," *Cell Death & Disease* 9, no. 6 (2018): 615, https://doi.org/10.1038/s41419-018-0648-0.

69. R. O. Hynes, "Integrins: A Family of Cell Surface Receptors," *Cell* 48, no. 4 (1987): 549–554, https://doi.org/10.1016/0092-8674(87)90233-9.

70. W. L. Lei, S. G. Xing, C. Y. Deng, X. C. Ju, X. Y. Jiang, and Z. G. Luo, "Laminin/β1 Integrin Signal Triggers Axon Formation by Promoting Microtubule Assembly and Stabilization," *Cell Research* 22, no. 6 (2012): 954–972, https://doi.org/10.1038/cr.2012.40.

71. O. Randlett, L. Poggi, F. R. Zolessi, and W. A. Harris, "The Oriented Emergence of Axons From Retinal Ganglion Cells Is Directed by Laminin Contact In Vivo," *Neuron* 70 (2011): 266–280, https://doi.org/10.1016/j.neuron.2011.03.013.

72. M. M. Riccomagno, L. O. Sun, C. M. Brady, et al., "Cas Adaptor Proteins Organize the Retinal Ganglion Cell Layer Downstream of Integrin Signaling," *Neuron* 81 (2014): 779–786, https://doi.org/10.1016/j.neuron.2014.01.036.

73. K. J. Tomaselli, D. E. Hall, L. A. Flier, et al., "A Neuronal Cell Line (PC12) Expresses Two Beta 1-Class Integrins-Alpha 1 Beta 1 and Alpha 3 Beta 1-That Recognize Different Neurite Outgrowth-Promoting Domains in Laminin," *Neuron* 5 (1990): 651–662, https://doi.org/10.1016/0896-6273(90)90219-6.

74. M. G. Vogelezang, Z. Q. Liu, J. B. Relvas, G. Raivich, S. S. Scherer, and C. ffrench-Constant, "Alpha4 Integrin Is Expressed During Peripheral Nerve Regeneration and Enhances Neurite Outgrowth," *Journal of Neuroscience* 21 (2001): 6732–6744.

75. R. N. Palchesko, L. Zhang, Y. Sun, and A. W. Feinberg, "Development of Polydimethylsiloxane Substrates With Tunable Elastic Modulus to Study Cell Mechanobiology in Muscle and Nerve," *PLoS One* 7 (2012): e51499, https://doi.org/10.1371/journal.pone.0051499.

76. C. Simitzi, A. Ranella, and E. Stratakis, "Controlling the Morphology and Outgrowth of Nerve and Neuroglial Cells: The Effect of Surface Topography," *Acta Biomaterialia* 51 (2017): 21–52, https://doi.org/10.1016/j.actbio.2017.01.023.

77. C. Hirsch and S. Schildknecht, "In Vitro Research Reproducibility: Keeping up High Standards," *Frontiers in Pharmacology* 10 (2019): 1484, https://doi.org/10.3389/fphar.2019.01484.